Fractional Models of Lithium-Ion Batteries with Application to State of Charge and Ageing Estimation

Jocelyn Sabatier[2(✉)], Franck Guillemard[1], Loic Lavigne[2], Agnieszka Noury[1], Mathieu Merveillaut[2], and Junior Mbala Francico[2]

[1] PSA Groupe, 2 Route de Gisy, 78943 Vélizy-Villacoublay, France [2] IMS, UMR 5218 CNRS, Bordeaux University,351 Cours de la Libération, 33405 Talence, France
jocelyn.sabatier@u-bordeaux.fr

Abstract. The lithium-ion batteries are currently used for a wide variety of mobile applications due to their high energy/power density and operating voltage. However, they also suffer from some limitations that force car manufacturers to associate them to a Battery Management System (BMS) that diagnoses and control the battery pack in real time. To carry out an accurate battery diagnosis, the BMS uses models of each cell in the pack. In this paper a two fractional models of lithium-ion cell are proposed. They result from several simplifications of an electrochemical model involving several partial differential equations. The very low number of parameters in the simpler proposed model permits their adjustment with a very simple procedure. It is then shown how this model can be used for State of Charge (SOC) and ageing estimation. As due to ageing cell and model behavior mismatch, a solution is proposed to define if the model parameters adjustment is required.

Keywords: Fractional models · Fractional differentiation · Lithium-ion batteries · SOC estimation · Ageing estimation

1 Introduction

Lithium-ion batteries have played a major role in the development of vehicle electrification since the 2000s. They are currently considered to be the most efficient technology in this market. However, they are the cause of a number of incidents and the safety of batteries presents a very important technical and societal challenge [1]. To manage this safety problem, but also to keep these new vehicles which are equipped with in good working order, car manufacturers must integrate a reliable electrical energy storage management [2]. That is why, state of charge (SOC) and state of health (SOH) estimators must be designed. To design these estimators, dynamical models of the battery pack can be a valuable tool.

K. Madani et al. (eds.), *Informatics in Control, Automation and Robotics*,
Lecture Notes in Electrical Engineering 430, https://doi.org/10.1007/978-3-319-55011-4_3

Many models exist in the literature for this kind of batteries such as electrochemical models [3–5], or purely electric models [6] or fuzzy models [7]. An extensive analysis on lithium ion batteries modeling is proposed in [8]. In this paper, fractional order models, models that can be described by fractional differential equations [25,26], are proposed. These models result from simplifications of an electrochemical model [4] that describes the battery behavior using partial differential equations. Such an approach makes it possible to express the parameters of the simplified model as a function of the dimensional and electrochemical constants of the lithium-ion cell. This model has thus an important physical meaning, unlike purely electric models proposed in the literature. Another interest is the introduction of fractional differentiation that helps to describe some parts of the model with a small number of parameters again directly related to the electrochemical parameters of the battery. As shown on several electrochemical devices [9–20], fractional differentiation permits to obtain models with a low number of parameters.

This paper, an extended version of the paper presented at the ICINCO'2016 conference, proposes two models. The first one, which is the most complex one, is no more based on partial differential equations and permits a description of the various internal variables of the cell. The second one, simpler, requires the adjustment of only 3 parameters and a nonlinear law with a very simple procedure. This last model is used to design a State Of Charge (SOC) and an ageing estimator. As due to ageing cell and model behavior mismatch, a solution is proposed to define if the model parameters adjustment is required.

2 Electrochemical Model Considered

The simplified model that will be presented in the sequel is based on lithium-ion electrochemical presented in [3,4] that results in Newman's modelling approach [5]. This model is a pseudo 2D based on a representation of the cell such as in Fig. 1.

In Fig. 1, the electrodes are seen as an aggregation of spherical particles (2D representation) in which the Li^+ ions are inserted. The first spatial dimension of this model, represented by variable x, is the horizontal axis. The second spatial dimension is the particle radius.

The cell is constituted of three regions (two electrodes and a separator) that imply four distinct boundaries at:

- $x = 0$: negative electrode current collector;
- $x \in]0; \delta_n[$: region 1, δ_n thickness negative carbon electrode (LixC6, MCMB...);
- $x = \delta_n$: negative electrode / separator interface;
- $x \in \rfloor\delta_n; \delta_n + \delta_{sep}\lfloor$: region 2, δ_{sep} thickness separator;
- $x = \delta_n + \delta_{sep}$: separator / positive electrode interface;
- $x \in \rfloor\delta_n + \delta_{sep}; L\lfloor$: region 3, δ_p thickness positive electrode made of LiCoO2;
- $x = L$: positive electrode current collector.

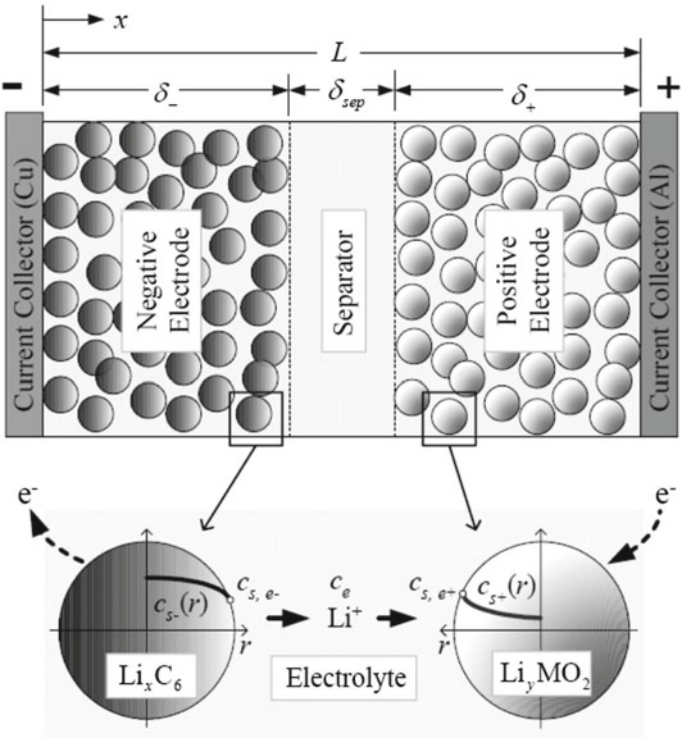

Fig. 1. Pseudo 2D model of a Lithium-ion cell [3,4]

The two electrodes are assumed electrochemically porous. Regions 1 and 3 are therefore constituted of a solid phase (electrode material) and a liquid phase (electrolyte).
The cell is supposed supplied by a current $I(t)$. The cell voltage denoted $U_{batt}(t)$ is defined by the relation

$$U_{batt}(t) = \phi_s(L,t) - \phi_s(0,t) - \frac{R_f}{A} I(t) \tag{1}$$

where $\phi_s(L,t)$ and $\phi_s(0,t)$ are respectively the positive electrode potential at abscissa $x = L$ and the negative electrode potential at abscissa $x = 0$; R_f denotes the contact resistance and A the electrodes surface. Note that all the parameters used in the following equations are defined in [3,4].

As described in [3,4], lithium concentration $c_s(x, r, t)$ evolution in the spherical particle of radius $r = R_s$, is supposed described by the diffusion law,

$$\frac{\partial c_s}{\partial t} = \frac{D_s}{r^2}\frac{\partial}{\partial r}\left(r^2 \frac{\partial c_s}{\partial r}\right) \quad \begin{cases} \frac{\partial c_s}{\partial r}\big|_{r=0} = 0 \\ D_s \frac{\partial c_s}{\partial r}\big|_{r=R_s} = \frac{-j^{Li}}{a_s F} \end{cases} . \tag{2}$$

Lithium concentration $c_e(x, t)$ in the electrolyte is modeled by:

$$\frac{\partial (\varepsilon_e c_e)}{\partial t} = \frac{\partial}{\partial x}\left(D_e^{eff}\frac{\partial}{\partial x}c_e\right) + \frac{1 - t_+^o}{F} j^{Li}, \tag{3}$$

with

$$\left.\frac{\partial c_e}{\partial x}\right|_{x=0} = \left.\frac{\partial c_e}{\partial x}\right|_{x=L} = 0. \tag{4}$$

Charge conservation in the solid phase of each electrode is defined by the Ohm's law:

$$\frac{\partial}{\partial x}\left(\sigma^{eff}\frac{\partial}{\partial x}\phi_s\right) - j^{Li} = 0 \tag{5}$$

with the following limit conditions at the current collectors

$$-\sigma_-^{eff}\left.\frac{\partial \phi_s}{\partial x}\right|_{x=0} = \sigma_+^{eff}\left.\frac{\partial \phi_s}{\partial x}\right|_{x=L} = \frac{I}{A}, \tag{6}$$

and the null current conditions at the separator:

$$\left.\frac{\partial \phi_s}{\partial x}\right|_{x=\delta_n} = \left.\frac{\partial \phi_s}{\partial x}\right|_{x=\delta_n+\delta_{sep}} = 0. \tag{7}$$

If $\phi_e(x, t)$ denotes the electrolyte potential, charge conservation in the electrolyte is defined by:

$$\frac{\partial}{\partial x}\left(\kappa^{eff}\frac{\partial}{\partial x}\phi_e\right) + \frac{\partial}{\partial x}\left(\kappa_D^{eff}\frac{\partial}{\partial x}\ln(c_e)\right) + j^{Li} = 0, \tag{8}$$

with the limit conditions

$$\left.\frac{\partial \phi_e}{\partial x}\right|_{x=0} = \left.\frac{\partial \phi_e}{\partial x}\right|_{x=L} = 0. \tag{9}$$

The four differential equations (2), (3), (5) and (8) that describe variables $c_{s,e}, c_e, \phi_s, \phi_e$, variations are linked by the Butler-Volmer equation

$$j^{Li} = a_s i_o\left\{\exp\left[\frac{\alpha_a F}{RT}\eta\right] - \exp\left[-\frac{\alpha_c F}{RT}\eta\right]\right\}. \tag{10}$$

In (10), j^{Li} is induced by overvoltage η, defined by the potential difference between the solid phase and the electrolyte and equilibrium thermodynamic potential U:

$$\eta = \phi_s - \phi_e - U. \tag{11}$$

The equilibrium potential U is a function of the solid phase concentration at the spherical particles. System input is the current $I(t)$ in Eq. (6). System output is the cell voltage given by relation (1).

3 From the Electrochemical Model to a Fractional Dynamic Model

The electrochemical model previously presented is not real time implementable in a car microcontroller. To solve this problem, as shown in [17–19], the following assumptions were proposed:

Assumptions 1.

- the solid phase potentials are supposed constants in the two electrodes (due to the low resistivity of electrode materials);
- the electrolyte potentials are constants in the two electrodes;
- current density j^{Li} is supposed constant in each electrode;
- Butler-Volmer equation is supposed linear on the cell operating current;
- lithium concentration in the separator is supposed a linear function of x around the initial value denoted $C_{ei}(x,0)$.

These assumptions have allowed the first simplified model presented in Fig. 2, in which electrochemical variables and parameters still appear (parameters physical meaning is often lost with an approach based on model reduction) but only based on differential equations. This model is thus easier to implement in a car controller than the electrochemical model. In Fig. 2 model, the transfer functions $H_{cei}(s)$, $i \in \{n,p\}$, link the current $I(s)$ to the electrolyte concentration at the abscissa δ_n and δ_p and are defined by:

$$H_{cei}(s) = \frac{C_e(\delta_i, s)}{I(s)} = \frac{K_{cei}}{1 + \frac{s}{\omega_{cei}}}. \tag{12}$$

Transfer functions $H_{csi,e}(p)$, $i \in \{n,p\}$, link the mean value of the lithium current density in electrode, denoted $J^{Li}_{i\_mean}(s)$, to the lithium concentration at the surface of the spherical particles. There are fractional transfer functions defined by:

$$H_{csi,e}(s) = \frac{c_{si,e}(s)}{J^{Li}_{i\_mean}(s)} = \frac{K_{1i}\left(1 + \frac{s}{\omega_{csei}}\right)^{0.5}}{s}. \tag{13}$$

Variables C_{si_0}, $i \in \{n,p\}$, in Fig. 2 denote the initial lithium concentration in the spherical particles. The linearized Butler-Volmer equation is defined by:

$$j^{Li}_{i\_mean} = \frac{a_{si} i_{0i} F}{RT}(\alpha_a + \alpha_c)\eta_i. \tag{14}$$

To obtain a simpler model, less microcontroller resources consuming, additional assumptions were proposed in [19].

Assumptions 2.

- lithium concentration in the electrolyte and in the separator is constant is supposed constant;

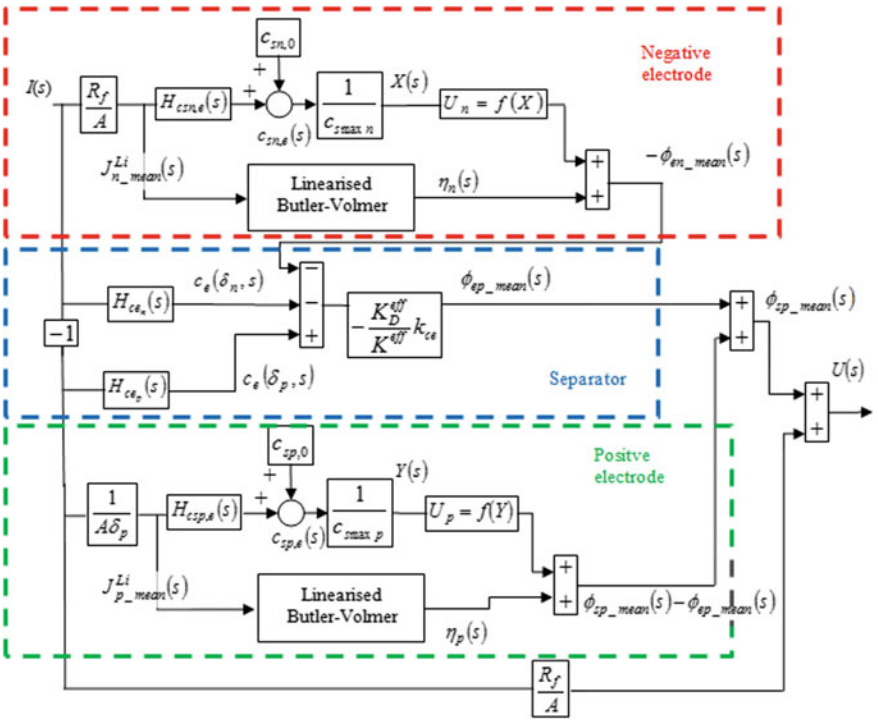

Fig. 2. Simplified model obtained

- the electrolyte potential is supposed constant at any SOC and such as: $\phi_e\,(x, Soc) = \phi_{e\_moy} = -0.1V$.

Using this last hypothesis, the part of Fig. 2 model that represents the negative electrode contribution can be removed. The resulting model is a single-electrode model represented in Fig. 3. This model is obtained by moving and consolidating some blocks and by introducing the following parameters:

$$\begin{cases} K_1 = \frac{K}{A\delta_p c_{s\,\max p}} \quad with \quad K = \frac{-3}{R_s F a_s} = \frac{1}{F\varepsilon_s} \\ K_2 = \frac{RT}{A\delta_p F(\alpha_a+\alpha_c)a_{sp}i_{0p}} + R_f \\ \omega_c = \frac{9D_{sp}}{R_s^2} \end{cases} . \tag{15}$$

4 Parameters Estimation

According to Fig. 3, only three parameters and a non-linear law are required to model the behaviour of a lithium-ion cell. These parameters can be obtained with the unique test represented by Fig. 4. This test consists in a series of discharges of 0.5 A.h since full charge (a decrease of around 7.1% on the SOC for each discharge from 100%). The interval between two discharges is large

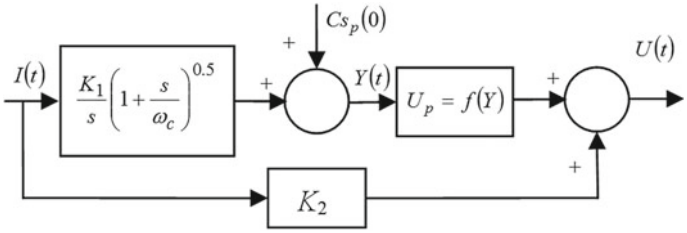

Fig. 3. Single-electrode model

enough to permit a measure of the open circuit voltage. The parameters estimation method presented in the sequel is repeated for several state of charge and several temperatures to check the dependence of the parameters to these two variables.

4.1 Open Circuit Voltage Law Identification

We suppose that the open circuit voltage can be described by the relation proposed in [22]:

$$U_p = U_p^0 + \frac{RT}{F}\ln\left(\frac{1-(Soc(\mathrm{x_{100p}}\text{-}\mathrm{x_{0p}})+\mathrm{x_{0p}})}{(Soc(\mathrm{x_{100p}}\text{-}\mathrm{x_{0p}})+\mathrm{x_{0p}})}\right) + \left\{\sum_{k=0}^{N_p} B_k \left[\begin{array}{l}(2\,(Soc\,(\mathrm{x_{100p}}\text{-}\mathrm{x_{0p}}) + \mathrm{x_{0p}}) - 1)^{k+1} \\ -\frac{2(Soc(\mathrm{x_{100p}}\text{-}\mathrm{x_{0p}})+\mathrm{x_{0p}})k(1-(Soc(\mathrm{x_{100p}}\text{-}\mathrm{x_{0p}})+\mathrm{x_{0p}}))}{(2(Soc(\mathrm{x_{100p}}\text{-}\mathrm{x_{0p}})+\mathrm{x_{0p}})-1)^{1-k}}\end{array}\right]\right\}. \quad (16)$$

Parameters B_k, x_{100p}, x_{0p} and U_p^0 associated to relation (16) are respectively and for the positive electrode, the interaction parameter in Redlich-Kister equation, lithium insertion ratios at SOC 100 and 0%, and the standard equilibrium potential. These parameters are obtained through the minimization of a quadratic criterion on the open circuit voltage measured on Fig. 4. For that, the open circuit voltage is measured at rest (3600s without any solicitation) after each current step that appears on Fig. 4. The variations of the open circuit voltage in relation to SOC are thus obtained and the corresponding curve is fitted by relation (16) through the minimization of a quadratic criterion.

4.2 Estimation of Parameter $\mathbf{K_2}$

Parameter K_2 models the instant resistance due to contact resistance and to activation phenomenon inside the electrodes. As s tends towards infinity, namely as time tends towards 0, model in Fig. 3 reduces to $U(s) = K_2 I(s) + U_0/s$ (U_0 being the open circuit voltage of the cell). As a consequence and as shown in Fig. 5, if a constant current is applied to the cell, a voltage drop whose magnitude is liked to parameter K_2 appears. This is why Fig. 4 shows that this parameter can be estimated on the cell voltage drop as a constant current is applied. K_2 is defined as the ratio of the voltage drop by the value of the current applied.

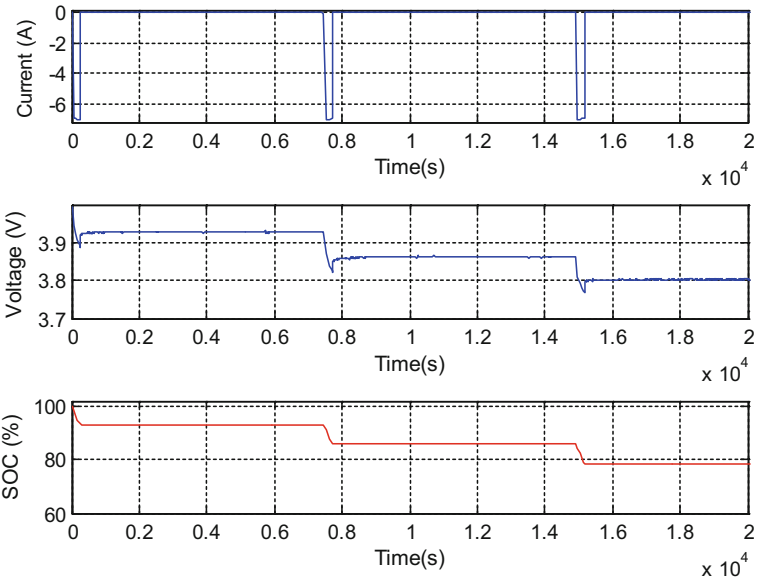

Fig. 4. Discharge test for parameters numerical values estimation of the single-electrode model (only the first discharges are shown on this figure)

4.3 Estimation of Parameter K_1

If $I(t)$ is a current step of amplitude A_{mp}, then Laplace transform of $Y(t)$ signal (see Fig. 3) is defined by:

$$Soc\,(s) = \frac{K_1}{s}\left(1 + \frac{s}{\omega_c}\right)^{0.5} \frac{A_{mp}}{s}. \tag{17}$$

Final value theorem applied to the derivative of $Y(t)$, leads to

$$\lim_{t\to+\infty} \frac{d\,(Y\,(t))}{dt} = \lim_{s\to 0} s^2 \frac{K_1}{s}\left(1 + \frac{s}{\omega_c}\right)^{0.5} \frac{A_{mp}}{s} = K_1 A_{mp}. \tag{18}$$

Relation (18) means that after some time characterized by the time constant $1/\omega_c$, (namely in the area in black in Fig. 5), if a constant current is applied to the cell, diffusion rate of Li^+ ions in the solid phase becomes sufficiently constant. This results in a linear variation of the cell voltage if the input current is not too high to avoid too rapid SOC variation (the open circuit voltage law can thus be assimilated to a straight line). This linear variation appears in Fig. 5 and this is why this figure defines the linear part of the step response as the time interval on which parameter K_1 can be estimated. Parameter K_1 is thus the slope (divided by Amp) of function $Y(t)$ on the interval shown in Fig. 5, as a current step is applied to the cell. Function $Y(t)$ can be estimated using the inverse of the open circuit voltage curve, parameter K_2, and signals $I(t)$ and $U(t)$ being known.

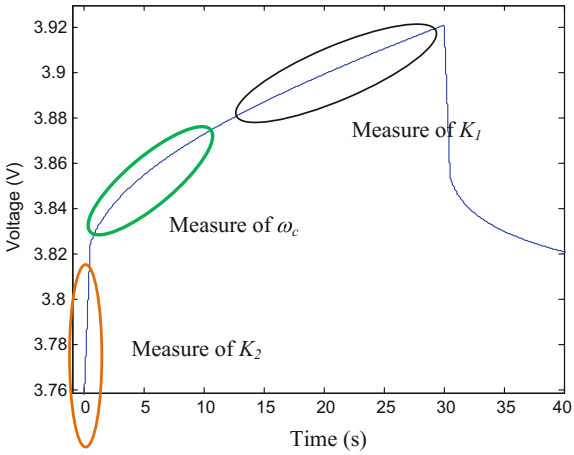

Fig. 5. Cell response to a step current and definitions of areas used for the identification of parameters K_1, K_2 and ω_c

4.4 Identification of Parameter ω_c

As shown in [19], if a step input current of magnitude A_{mp} is applied to model in Fig. 4, variable $w(t)$ is defined by:

$$w(t) = \frac{K_1 A_{mp}}{\omega_c} \left(\begin{array}{l} 0.5erf\left((\omega_c t)^{0.5}\right) \\ +t\omega_c erf\left((\omega_c t)^{0.5}\right) + \frac{0.5642(\omega_c t)}{e^{\omega_c t}} \end{array} \right). \tag{19}$$

Signal $w(t)$ can be obtained with a measure of $U(t)$ using the parameter K_2 computed in Sect. 4.2, value of c_{sp0} and using the open circuit law obtained in Sect. 4.1. Introducing function $z(t) = w(t)/t$, at a time

$$t_0 = \frac{k}{\omega_c} \quad \text{with} \quad k \in R^+, \tag{20}$$

then

$$z(t_0) = \frac{K_1 A_{mp}}{k} \left(\begin{array}{l} 0.5erf\left(\left(\frac{1}{k}\right)^{0.5}\right) \\ +\frac{1}{k} erf\left(\left(\frac{1}{k}\right)^{0.5}\right) + \frac{0.5642\left(\frac{1}{k}\right)}{e^{\frac{1}{k}}} \end{array} \right). \tag{21}$$

Thus, from the graph of $z(t)$, t_0 is the time at which $z(t)$ is given by relation (21), and from relation (20), the value of ω_c is obtained. Note that k must be chosen such that at time t_0 the batteries state of charge is close to its initial value and in the time interval on which the step response curvature appears (see Fig. 5).

5 Model Validation

To validate the single electrode model and its associated parameters estimation method, the charge cycle of Fig. 6 is applied to the model and to a 7 Ah real

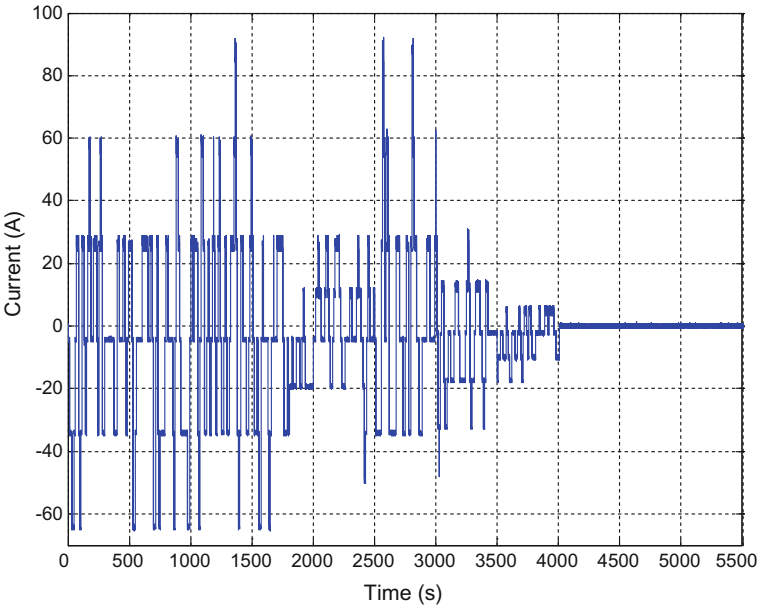

Fig. 6. Current cycle

lithium ion cell. During this cycle, state of charge cell varies form 80 to 20%. Figure 7 shows a comparison of the cell voltage and of the model response. The relative error between cell voltage and model response is also shown in Fig. 7. These figures show that the model is very efficient (less than 1.5% error). When the state of charge is below 20%, error mean value increases but remains low (less than 1%). Additional analyses can be found in [19].

6 State-of-Charge Estimation

Li-ion battery packs have to work together with reliable Battery Management Systems (BMS) to ensure their optimal and safe use. Among the tasks ensured by the BMS, State-Of-Charge (SOC) estimation is of crucial importance. To obtain this information that cannot be measured, an output feedback based observer was used involving the cell model of Fig. 3 is proposed. The Li-ion cell is parameterized on the basis of a SAFT VL6P lithium-ion cell according to the techniques exposed in Sect. 4.

For implementation issues, the transfer function $K_1 \left(1 + s/\omega_c\right)^{0.5}/s$ in Fig. 3 is split into the sum of two transfer functions K_1/s and $H(s)$, with:

$$H\left(s\right) = \frac{K_1}{s}\left[\left(1 + \frac{s}{\omega_c}\right)^{0.5} - 1\right]. \tag{22}$$

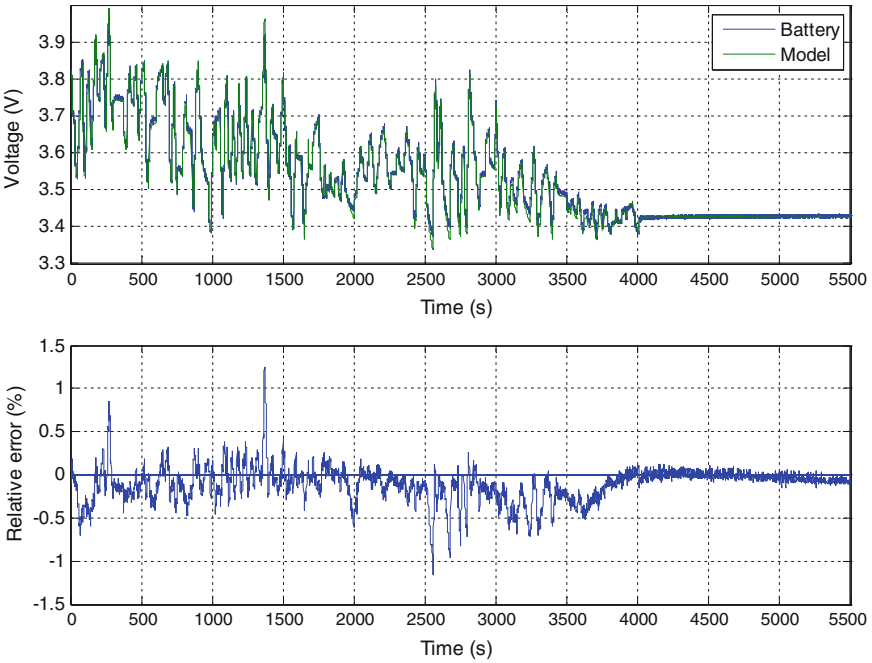

Fig. 7. Cell voltage variations / model response comparison for a current cycle and relative error T = 25° C

In order to adopt a linear approach in the observer design, the OCV is locally reduced to its first order approximation and represented by a SOC depending gain G_0. The controller in the observer is then designed to ensure satisfactory performance for all the G_0 gains. To take into account these gain variations, a CRONE controller can be designed [23] [24]. The model voltage and SOC Laplace transforms are thus given by:

$$U(s) = (SOC(s) + I(s) H(s)) G_0 + I(s) K_2, \tag{23}$$

and:

$$SOC(s) = I(s) \frac{K_1}{s} + SOC_0(s) \quad \text{where} \quad SOC_0(s) = \frac{SOC_0(0)}{s}. \tag{24}$$

The input $I(s)$ and output $U(s)$ are respectively the cell current and voltage. The estimation errors are noted $\varepsilon_U = U_{cell} - U$ for the voltage and $\varepsilon_{SOC} = SOC - \hat{SOC}$ for the SOC.

As shown by Fig. 8, to reduce ε_{SOC}, the model/cell output error can be used to modify the model SOC through the controller C_{SOC}.

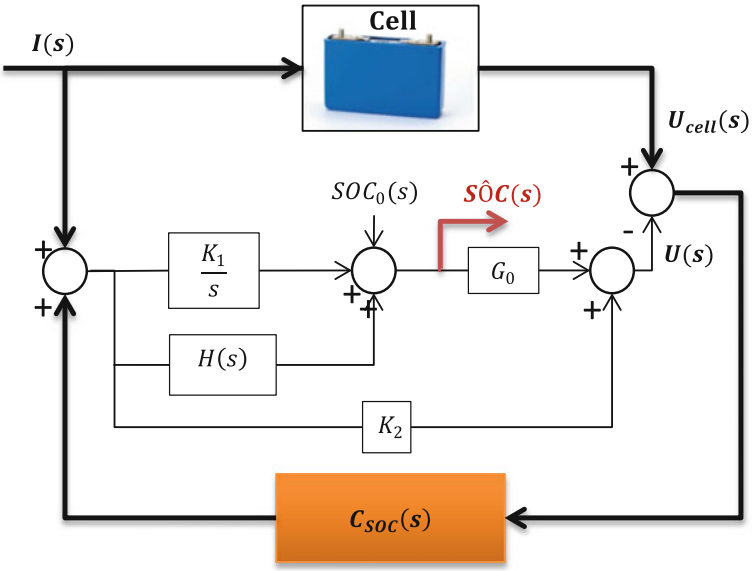

Fig. 8. SOC feedback observer

The estimated voltage and SOC are then given by

$$\begin{cases} \hat{U}(s) = \left(S\hat{O}C(s) + I(s)H(s)\right)G_0 + I(s)K_2 \\ \varepsilon_U(s) = G_0\varepsilon_{SOC}(s) \\ S\hat{O}C(s) = I(s)\frac{K_1}{s} + S\hat{O}C_0(s) + C_{SOC}(s)\varepsilon_U \end{cases}, \tag{25}$$

which gives:

$$SOC(s) = \frac{1}{1 + G_0 C_{SOC}(s)}\Delta SOC_0(s). \tag{26}$$

The equation linking the SOC estimation error to the voltage estimation error in (26) shows that, as long as the model is well parameterized:

$$\varepsilon_{U=0} \Rightarrow \varepsilon_{SOC} = 0. \tag{27}$$

The designed observer has been validated using the cell real SOC and voltage response to a dynamic hybrid drive cycle. Note that the << real >> SOC results in coulomb counting validated at the end of each solicitation and after the cell relaxation, by comparison of the real open circuit voltage versus the simulated one. The controller $C_{SOC}(s)$ is a CRONE controller [23,24].

Figure 9 shows the estimation produced by the observer of Fig. 8. The initial SOC for the cell was 80% and the initial SOC in the observer was 0. The measurements were done at temperature $T = 25°$ C. The resulting SOC estimation absolute error is represented in Fig. 9. This figure highlights the accuracy of the estimated SOC with an absolute error less than 3%.

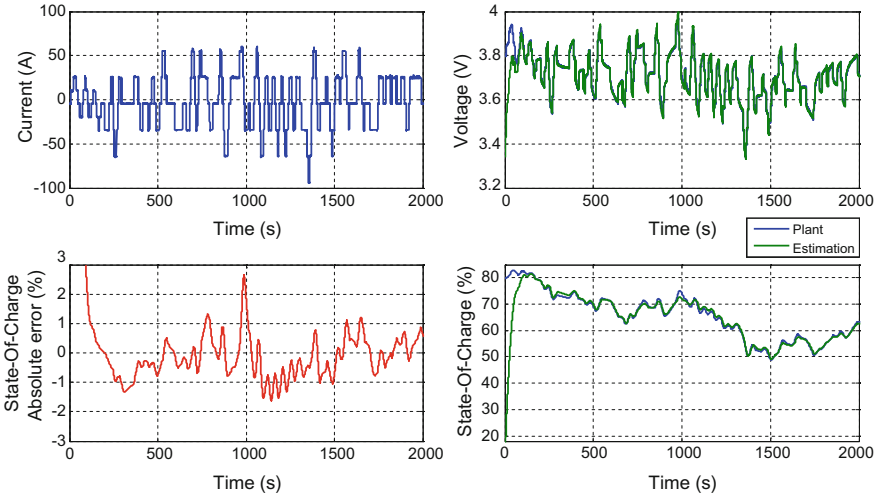

Fig. 9. SOC feedback observer validation, $T = 25°\mathrm{C}$

7 Aging Monitoring Through Open Circuit Voltage (OCV) Curve Modelling and Adjustment

At battery aging, the OCV curve changes, as OCV reflects battery aging and performance degradation [27]. The impact of aging on cell equilibrium voltage is analyzed in [28]. This change distorts the estimator if nothing is done to adjust the curve law. Taking into the underlying physical phenomenon of lithium-ion intercalation process, permits an analytical description of the OCV curve and the implementation of accurate estimation methods for both SOC and State of Health (SOH).

Expansion of relation (23) shows that OCV can be defined by the following polynomial:

$$U = \sum_{k=0}^{N} D_k^{init} SOC^k. \tag{28}$$

To take into account ageing impact on the OCV, [21][23] demonstrate that a parameter $\alpha\,(age)$, depending on cell age, can be introduced thus leading to:

$$U = \sum_{k=0}^{N} D_k \left(\alpha\,(age)\, SOC\,(t) + 1 - \alpha\,(age)\right)^k. \tag{29}$$

To validate this approach, an OCV curve for a new cell is first fitted by relation (28) (see blue curve in Fig. 10). After ageing, the cell OCV is measured and fitted, though optimization of parameter $\bar{\alpha}\,(age)$, by relation (29) (see orange curve in Fig. 10). Figure 10 shows the efficiency of the parametrization given by relation (29) and also shows that the proposed optimization leads to a reliable reconstruction of the OCV curve over a wide range of SOC.

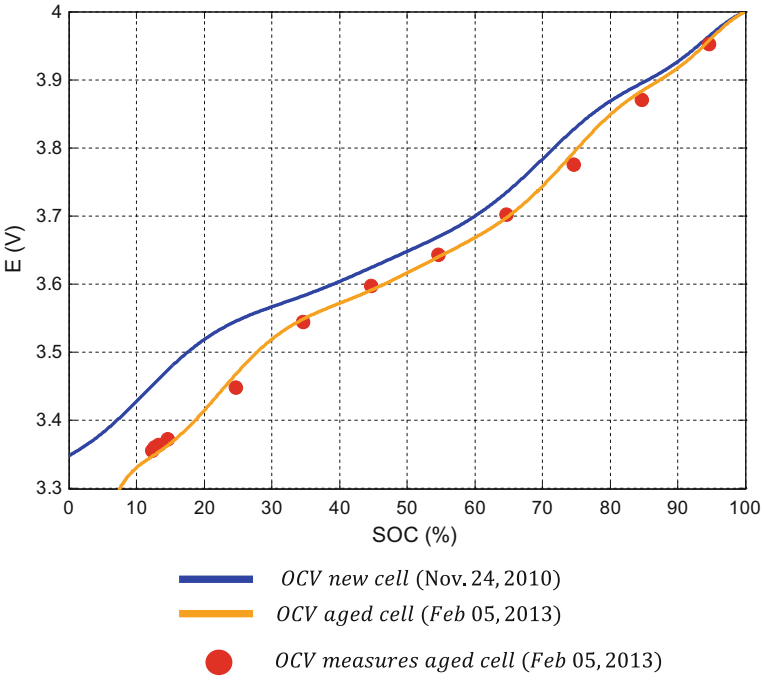

Fig. 10. Identification of the OCV after two years calendar ageing

Several other tests have been done for various cells at various ageing to evaluate parameter $\alpha\,(age)$ variations according to cell aging. These analysis have revealed that the higher is a cell age, and the higher is $\alpha\,(age)$. Thus parameter $\alpha\,(age)$ permits the OCV curve adjustment as cell aging and can also be viewed as a SOH indicator or a capacity fade indicator. As parameter K_1 is directly linked to the cell capacity, it can be adjusted with parameter $\alpha\,(age)$ as cell ageing.

8 Model Parameter Adjustment as Ageing

Model proposed in Sect. 3 allows an accurate characterization of the dynamic behavior of the cell at a given time. Section 7 has shown that this accuracy is affected by ageing as OCV curve is modified by ageing. Parameters K_1, K_2 and ω_c in this model will also gradually become inadequate, resulting in drifts in the accuracy of the algorithms using it (for instance SOC estimation). It is therefore essential to have a method evaluating the validity of the model of a cell and indicating, the need to recalibrate it.

A method consists in measuring the errors (deviations) between the voltage cell $U_{cell}(t)$ and the voltage model $U(t)$ on the same time interval and integrating this error on all the samples (here N samples at time t_k) in order to have an overall measurement of the error. Numerically, this leads to the following

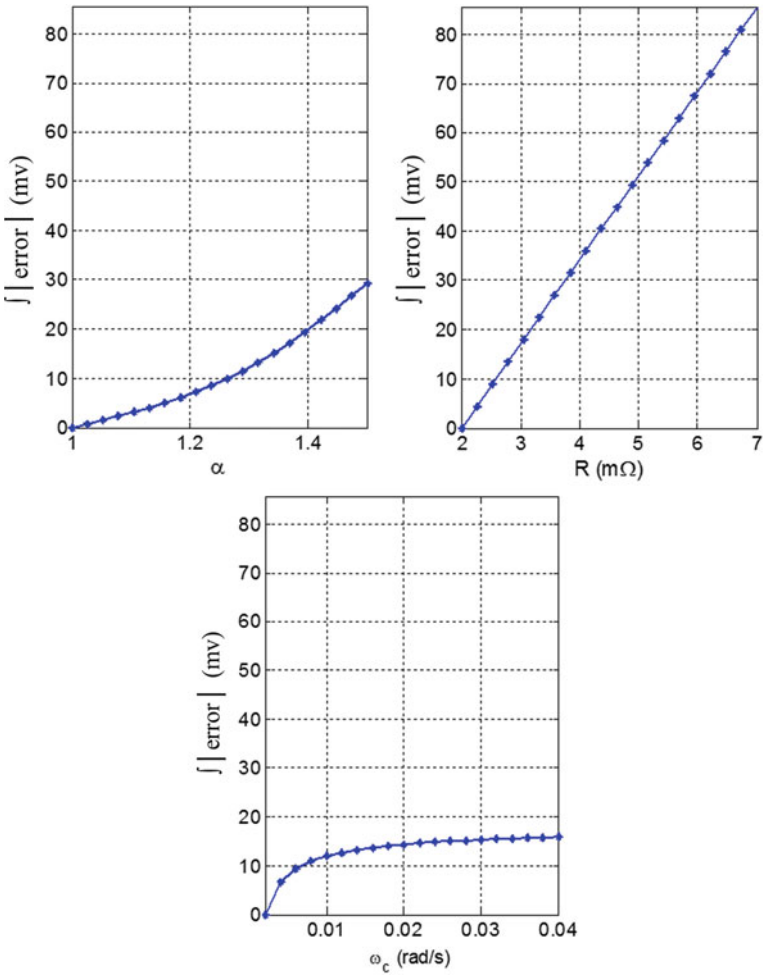

Fig. 11. Computation of ε_U for various behavioural gaps between a cell and its model

calculation:

$$\varepsilon_U = \frac{1}{N}\sum_{k=1}^{N} |U_{cell}(t_k) - U(t_k)|. \tag{30}$$

If this error exceeds a user fixed threshold, the model can be considered as mismatched and the calibration method described in Sect. 4 must be restarted. To illustrate the idea, relation (30) is applied using voltages computed from the single electrode model of Fig. 3 on a time interval of 400 s with a sampling period of 0.01s. The model parameters are supposed given by:

- $\alpha(age) = 1$;
- $\omega_c = 2.10^{-3}$rd/s ;

- $K_1 = 0.00194$
- $K_2 = 2.10^{-3}\Omega$.

The cell voltage variations are also computed with this model but using the following parametric variations (to simulate the mismatch of the model and the cell behaviour):

- $\alpha\,(age) \in [1,\ 1.1,\ 1.2,\ 1.3,\ 1.4,\ 1.5]$;
- $\omega_c = 10^{-3}\text{x}\,[2,\ 9.6,\ 17.2,\ 24.8,\ 32.4,\ 40]$ rd/s;
- $K_1 = (7 - 0.5\alpha\,(age))\,/3600$
- $K_2 = 10^{-3}\text{x}\,[2,\ 4,\ 6,\ 8,\ 10]\,\Omega$;

Figure 11 shows that the higher is the difference between the dynamic behaviour of the cell and of the model, and the higher is the value of. It can be considered as a mismatch indicator, which imposes the model parameter adjustment using method proposed in Sect. 4, over a user defined level.

9 Conclusion

Fractional differentiation and fractional models are now widely used to model systems that exhibits long memory behaviours or systems in which diffusion phenomena take place. This is exactly the case with lithium ion batteries with the diffusion of Li^+ ion inside the electrodes. This paper thus proposes two models for a lithium-ion cell in which fractional transfer functions are used and that are deduced from an electrochemical model after several assumptions. Due to the approach used, several internal variables in the first model (the most complex), are real electrochemical variable and its parameters are directly correlated to the dimensional and electrochemical constants of the lithium-ion cell. The second model (the simpler one) only requires the tuning of three parameters and a nonlinear law (to model the cell open circuit voltage). This model can be easily implemented in a car controller and its accuracy is proved. It is used to design a state of charge and an ageing indicator.

The authors are now currently working to associate a thermal model to the proposed models.

Acknowledgements. This work took place in the framework of the Open Lab Electronics and Systems for Automotive combining IMS laboratory and PSA Groupe company.

References

1. Farrington, M.D.: Safety of lithium batteries in transportation. J. Power Sources **96**(N° 1), 260–265 (2001)
2. Chatzakis, J., Kalaitzakis, K., Voulgaris, N.C., Manias, S.N.: Designing a new generalized battery management system. IEEE Trans. Ind. Electron. **50**(5), 990–999 (2003)

3. Kandler, A.S., Rahn, D.C., Wang, C.: Model-Based electrochemical estimation and constraint management for pulse operation of lithium ion batteries. IEEE Trans. control Syst. Technol. **18**(N° 3), 654–663 (2010)
4. A. S. Kandler, Electrochemical Modeling, Estimation and Control of lithium-ion batteries, Pennsylvania University Ph.D. thesis (2006)
5. Newman, J., Thomas-Alyea, K.E.: Electrochemical Systems, 3rd edn. Wiley (2004)
6. Buller, S., Thele, M.: De Doncker R. W. A. A., Karden E., Impedance-Based simulation models of supercapacitors and Li-Ion Batteries for power electronic Applications. IEEE Trans. Ind. Appl. **11**(3), 742–747 (2005)
7. Singh, P., Vinjamuri, R., Wang, X., Reisner, D.: Design and implementation of a fuzzy logic-based state-of-charge meter for Li-ion batteries in portable defibrillators. J. Power Sources **162**, 829–836 (2006)
8. Sikha, G., White, R.E., Popov, B.N.: A mathematical model for lithium-ion battery/electrochemical Capacitor hybrid System. J. Electrochem. Soc. A1682–A1693 (2005)
9. Sabatier, J., Aoun, M., Oustaloup, A., Gregoire, G., Ragot, F., Roy, P.: Fractional system identification for lead acid battery sate charge estimation. Signal Process. J. **86**(N° 10), 2645–2657 (2006)
10. Cugnet, M., Laruelle, S., Grugeon, S., Sahut, B., Sabatier, J., Tarascon, J.M., Oustaloup, A.: A mathematical model for the simulation of new and aged automotive lead-acid batteries. J. Electrochem. Soc. **156**(12), A974–A985 (2009)
11. Cugnet, M., Sabatier, J., Laruelle, S., Grugeon, S., Chanteur, I., Sahut, B., Oustaloup, A., Tarascon, J.-M.: A solution for lead-acid battery global state estimation. ECS Trans. **19**(n° 25), 77–88 (2009)
12. Bertrand, N., Sabatier, J., Briat, O., Vinassa, J.M.: Fractional Non-Linear modelling of ultracapacitors. Commun. Nonlinear Sci. Numer. Simul. **15**(5), 1327–1337 (2010)
13. Sabatier, J., Cugnet, M., Laruelle, S., Grugeon, S., Sahut, B., Oustaloup, A., Tarascon, J.M.: A fractional order model for lead-acid battery crankability estimation. Commun. Nonlinear Sci. Numer. Simul. **15**(5) (2010)
14. Cugnet, M., Sabatier, J.: S. laruelle, S. Grugeon, B. Sahut, A. Oustaloup, J.M. Tarascon - Lead-acid battery fractional modeling associated to a model validation method for resistance and cranking capability estimation. IEEE Trans. Ind. Electron. **57**(3), 909–917 (2010)
15. Bertrand, N., Sabatier, J., Vinassa, J.M., Briat, O.: Embedded fractional nonlinear supercapacitor model and its parametric estimation method. IEEE Trans. Ind. Electron. **57**(12), 3991–4000 (2010)
16. Bertrand, N., Sabatier, J., Briat, O., Vinassa, J.M.: An implementation solution for fractional partial differential equations. Math. Probl. Eng. (2013). available on line at www.hindawi.com/journals/mpe/aip/795651.pdf
17. Sabatier, J., Merveillaut, M., Francisco, J., Guillemard, F.: Lithium-ion batteries modelling involving fractional differentiation. J. power sources, J. Power Sources **262C**, 36–43 (2014)
18. J.M. Francisco, J. Sabatier, L. Lavigne, F. Guillemard, M. Moze, M. Tari, M. Merveillaut, A. Noury.: Lithium-ion battery state of charge estimation using a fractional battery model, IEEE International Conference on Fractional Differentiation and its Applications, 23–25 (June 2014), Catania, Italy
19. J. Sabatier, J. Francisco, F. Guillemard, L. Lavigne, M. Moze, M. Merveillaut.: Lithium-ion batteries modelling: a simple fractional differentiation based model and its associated parameters estimation method, Signal Processing, pp. 290–301 (2015)

20. Lavigne, L., Sabatier, J., Mbala Francisco, J., Guillemard, F., Noury, A.: Lithium-ion open circuit voltage (OCV) curve modelling and its ageing adjustment. J. Power Sources (n° 324), 694–703 (2016)
21. L. Lavigne, J. Sabatier, J. Mbala Francisco, F. Guillemard, A. Noury.: Lithium-ion Batteries Aging Monitoring Through Open Circuit Voltage (OCV) Curve Modelling and Adjustment, 12th International Conference on Informatics in Control, Automation and Robotics, ICINCO 29–31 (July 2016), Lisbon, Portugal
22. Karthikeyan, D.K., Sikha, G., White, R.E.: Thermodynamic model development for lithium intercalation electrode. J. power sources (N° 185), 1398–1407 (2008)
23. Sabatier, J., Oustaloup, A., Garcia, A., LANUSSE, P.: CRONE control: Principles and extension to time-variant plants with asymptotically constant coefficients. Nonlinear Dyn. **29**(N° 1–4), 363–385 (2002)
24. Oustaloup, A., Lanusse, P., Sabatier, J., Melchior, P.: Crone control : principles, extensions and applications. J. Appl. Nonlinear Dyn. **2**(N°3), 207–223 (2013)
25. Agrawal, O.P., Machado, J.A.T., Sabatier, J.: Nonlinear Dynamics: introduction. Nonlinear Dyn. **38**(N° 1–4), 1–2 (2004)
26. Podlubny, I.: Fractional Differential Equations. Academic Press, Mathematics in Sciences and Engineering (1999)
27. Roscher, M.A., Assfalg, J., Bohlen, O.S.: Detection of utilizable capacity deterioration in battery systems. IEEE Trans. Veh. Technol. **60**, 98–103 (2011)
28. Schmidt, J.P., Tran, H.Y., Richtera, J., Ivers-Tifféea, E., Wohlfahrt-Mehrensb, M.: Analysis and prediction of the open circuit potential of lithium-ion cells. J. Power Sources **239**, 696–704 (2013)